

# Severity Differentiation and Detection of Glaucoma using Pulikulam Cattle Optimization Algorithm (PCOA)-Based CNN in Retinal Fundus Image

**S. Sheeba Jeya Sophia\***

Assistant Professor/ECE, Kalasalingam Academy of Research and Education,  
Anand Nagar, Krishnankoil, Virudhunagar District – 626126, India  
[\*Corresponding author]

**S. Diwakaran**

Associate Professor/ECE, Kalasalingam Academy of Research and Education,  
Anand Nagar, Krishnankoil, Virudhunagar District – 626126, India

## Abstract

Glaucoma, a debilitating eye condition, poses a significant threat to vision by damaging optic nerve fibers and astrocytes irreversibly. Early detection of glaucoma is crucial for timely intervention and preservation of vision. Retinal image-based detection methods offer a non-invasive approach for early diagnosis, which can alleviate the burden on ophthalmologists and improve patient outcomes. In this study, we propose a novel method called the Pulikulam Cattle Optimization Algorithm (PCOA) for glaucoma detection using retinal fundus images. The PCOA algorithm is employed to optimize the weights of a Convolutional Neural Network (CNN) classifier, enhancing its accuracy and efficiency in detecting glaucomatous features. The fitness function of the PCOA algorithm aims to minimize error values, leading to the identification of optimal solutions for glaucoma detection. The resulting optic disc area extracted from retinal images serves as a crucial indicator for distinguishing between healthy and glaucomatous eyes. We conducted comprehensive evaluations using diverse datasets, demonstrating well-organized clustering, precise classification, and superior performance compared to existing methods. Our proposed approach achieved accuracy levels exceeding 95%, underscoring its effectiveness in glaucoma detection. The findings of this study contribute to advancing glaucoma detection technology and hold promise for improving clinical outcomes and patient care.

## Keywords

Glaucoma, Retinal images, Clustering, Cattle optimizer with CNN classification

## INTRODUCTION

According to the WHO (World Health Organization) [1], glaucoma causes close to 12% of all incidents of blindness globally. In 2010, it was estimated that 60.5 million people worldwide suffered from glaucoma, and by 2020, it's expected that figure will reach 80 million [2]. In general, elderly adults are more likely to develop glaucoma, particularly those who have severe nearsightedness, diabetes, or high blood pressure. Glaucoma gradually weakens the optic nerve, which carries visual data coming from the eye to the brain. Early-stage glaucoma rarely impairs vision; therefore patients frequently are unaware of it. The loss of peripheral vision brought on by advanced glaucoma may result in permanent blindness. However, an early diagnosis and the right treatment can halt the progression of the condition and stop vision loss.

Early diagnosis of this irreversible glaucoma problem is important as a result [3]. As examples of several glaucoma kinds, consider the following: open-angle, angle-closure, normal tension, and congenital [4]. Before making a glaucoma diagnosis, important factors such as tonometry, perimetry, ophthalmoscopy, pachymetry, and gonioscopy have to be investigated. The tests for visual field loss, intraocular pressure (IOP), and an ophthalmoscopy assessment of the optic nerve head (ONH) are then used to make the glaucoma diagnosis [5] for patients. Glaucoma can be detected with digital fundus cameras, optical coherence tomography (OCT), IOP readings, ONH assessments, retinal nerve fiber layer (RNFL), and visual field abnormalities [4]. IOP quickly increases as a consequence of a drainage system problem in the eyes. After

that, the fluid pressure in the eyes gradually rises; as a result, it harms the optic nerve [6] and results in irreversible visual loss [7], which produces glaucoma. Fig. 1 depicts the drainage canal is blocked and buildup of fluid.

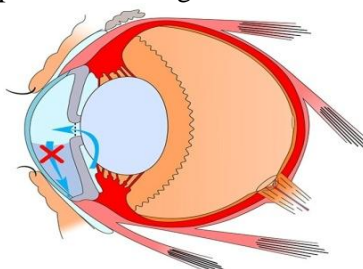


**Fig. 1** Glaucoma

In addition, RNFL destruction, which results in decreased RNFL thickness, is one of the primary risk factors of glaucoma disease [8]. Additional potential causes of the glaucoma condition include the concurrent functional cessation of the visual field, ONH, nerve fiber layer, structural changes, and other factors [9].

Therefore, to help with the early diagnosis of the condition, regular eye exams are required for those who may have glaucoma. During an eye exam, an ophthalmologist shall manually assess a patient's retinal image to check for the existence of glaucoma symptoms. Manually analyzing retinal images can take a lot of time [10]. Highly skilled ophthalmologists should also review the photos to guarantee the precision of the performed diagnosis [11].

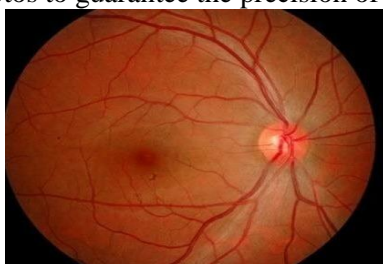


**Fig. 2** Retinal Fundus Image

Ophthalmologists can distinguish among healthy and unhealthy retinas [13] using one of the most important noninvasive glaucoma diagnostic tools [12]. The fact that retinal fundus images are typically easy to produce in clinical settings is their greatest advantage. Then, information from digital image research is extrapolated [14] to identify eye conditions associated with glaucoma. In order to successfully detect this illness, numerous clustering and classification progression approaches are used. The paper's contribution, in a nutshell, is as follows:

- This work examines various important contributions and introduced a new optimizer called pulikulam cattle optimizer along with the tuning of neural network model (CNN) and achieving simulation performance improvement.
- It considers pulikulam cattle optimization (PCOA) is proposed to tune the learning rate of the Back propagation approach and activation perspectives.
- The workput forward in what way the bonding among swarm optimization module and deep learning can be strengthened.

The relevant studies are described in next section. The submitted methodology, new model and their implemented concepts with outcomes are provided in the well-ordered sections.

## RELATED REVIEWS

Glaucoma constitutes one of the leading causes of irreversible blindness in our ageing society [15]. Chronic neuropathy alters the optic disc both internally and externally, producing structural damage to the optic nerve fibers that ultimately results in functional vision loss. Glaucoma is associated with specific changes in the optic nerve head (ONH), often referred to as the optic disc [16]. Throughout a clinical evaluation and optic disc photo analysis, ophthalmologists evaluate the ONH while looking for recognizable changes, such as generalized or focal neural rim thinning.

CNN (Convolutional neural networks) and deep learning models more specifically are establishing new benchmarks in the field of medical image processing. Numerous healthcare applications, including the diagnosis of pneumonia on chest CT [18] and the grading of skin cancer at the dermatologist level [17] use these models. The primary focus of research in ophthalmology has been on CNNs' potential for early detection of serious eye diseases like cataract [21], age-related macular degeneration [20], and diabetic retinopathy [19] using inexpensive color fundus photos and, to a lessened range, optical coherence tomography (OCT) scans.

Deep learning-based assessments may aid in reducing the false positive rate while addressing the issue of under diagnosis of glaucoma [22]. Successes have been documented in the area of automated glaucoma diagnosis [23] and glaucoma associated indicators [24] from fundus images using CNNs. Those results emerged at the expense of less knowledge regards the predictive model's method of decision-making because picture features are no longer manually developed and selected. Fostering trust in the prospective use of deep learning for medical diagnosis requires transparency in decision-making, which is also referred to as CNN explain ability.

However, CNNs might perform less well and be unable to differentiate between different glaucoma severities levels due to the stochastic choice of hyper-parameters. The hyper-parameter's value controls the rate of convergence and steers the approach to the desired minimum or maximum [25]. The optimization method offers a higher level of choice of parameters precision than all common approaches, but it may lead to high amounts of computer complexity. Many swarm-based optimization techniques [25] include two brand-new heuristic algorithms that work well as optimizers. Thus, the Chicken Swarm [28] Optimization procedure is combined with a similar approach. By emulating the hierarchical structure of the chicken swarm and its behaviors, including those of roosters, hens, and chicks, CSO may effectively obtain the chickens intelligence from swarms to resolve problems.

In our approach, we tried to reduce the loss function in CNN model with the help of cattle optimizer. This can reduce the error rate much better than the previously studied optimizers. Thus, the way of accurate location of glaucoma disease can be detected effectively, when compared to the conventional approaches [30-32].

## GENERAL CONCEPTS

### 1. *Glaucoma Detection:*

Glaucoma is a leading cause of blindness globally, necessitating early detection to prevent irreversible vision loss. Various diagnostic tools, including tonometry, perimetry, and ophthalmoscopy, aid in identifying glaucoma symptoms.

### 2. *Retinal Fundus Images:*

Retinal fundus images serve as crucial diagnostic tools for glaucoma detection due to their non-invasive nature and ease of production in clinical settings. Ophthalmologists analyze these images to identify abnormalities associated with glaucoma.

### 3. *Challenges in Manual Analysis:*

Manual analysis of retinal images by ophthalmologists is time-consuming and requires high levels of skill and expertise. Automation of this process using computational techniques can improve efficiency and accuracy in glaucoma diagnosis.

### 4. *Role of Clustering and Classification:*

Computational techniques such as clustering and classification play a significant role in automated glaucoma detection. These techniques extract relevant features from retinal images and classify them as healthy or diseased, aiding in early diagnosis and intervention.

### 5. *PCOA:*

The Pulikulam Cattle Optimization Algorithm (PCOA) is introduced as a novel optimization method for enhancing glaucoma detection using retinal fundus images. Inspired by the dietary habits of cattle, PCOA optimizes the weights of Convolutional Neural Network (CNN) classifiers to improve accuracy and efficiency in glaucoma detection.

### 6. *PCOA Methodology:*

PCOA optimizes the learning rate of the Back propagation algorithm and activation perspectives in CNN classifiers, strengthening the bond between swarm optimization and deep learning techniques. By minimizing error values, PCOA identifies optimal solutions for glaucoma detection, leveraging insights from nature to enhance computational efficiency.

## GENERAL METHODOLOGY

The common architecture obtained from the previous work [29] is observed and adapted the new optimization module named as pulikulam cattle optimization algorithm. The overall block diagram of the proposed model is drawn in the below Fig. 1.

Three local sub-nets from the CNN framework are used. The three sub-nets consist of a sub-net for predicting ROI attention, a sub-net for locating problematic areas combined with the pulikulam cattle optimization algorithm, and a sub-net for classifying glaucoma. The first sub-net predicts the region of glaucoma to be given to the second sub-net by generating an attention map. The extracted attention maps and features are used by the second sub-net to identify the glaucoma area. The third sub-net divides the input image into glaucoma cases with varying degrees of severity and glaucoma-negative cases. A hybrid optimization strategy is suggested for second sub-net in order to adjust the loss function's hyper-parameters for the three-tiered CNN structure as mentioned in below Fig. 3.

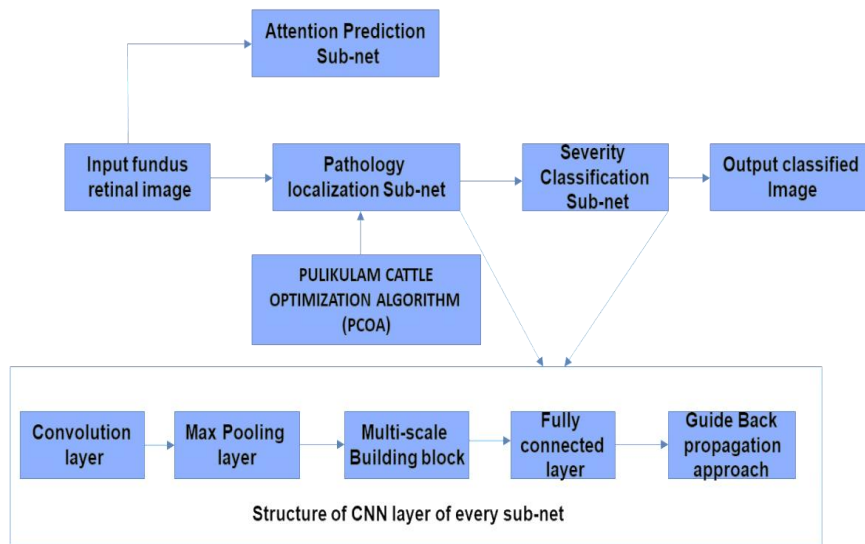


Fig. 3 The schematic figure of the proposed PCOA-CNN

## PROPOSED CNN WITH OPTIMIZER

### Pulikulam Cattle Optimization algorithm (PCOA)

The pattern of the cattle in the paddock serves as the inspiration for the livestock optimization method. The behavior of cattle in the paddock, or the area enclosed inside a specified space can serve as the basis for this algorithm. First, the cattle forage for food in its immediate vicinity and quickly graze the entire covering area. By acting in this manner, it will totally graze the area during its prime grazing season without leaving a single food inside the paddock. For multi-objective problems, this behavior is used to search the solution in a search space without overlooking any potential solutions. The paddock that may be connected to the limitations or constraints created with regard to situations with several objective functions to establish an upper and lower bound for solutions that are appropriate for the issue as depicted in below Fig. 4.

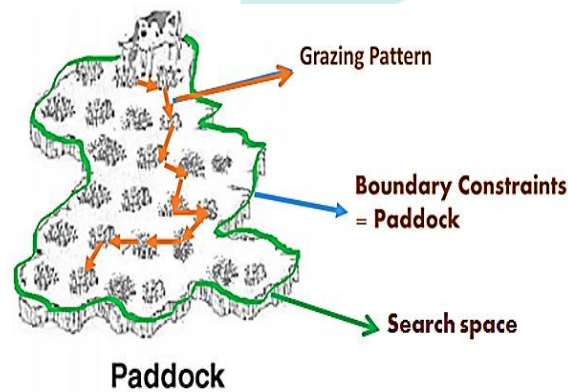


Fig. 4 Cattle grazing pattern within paddock

Only the paddock, which is seen as a space for solution searching, is used for cattle grazing. Paddock in relation to the limitations created to determine whether the chosen solution is accurate and ideal. In order to find food, cattle graze haphazardly and quickly throughout the paddock. It has to do with locating the greatest and most suitable solution. Additionally, the algorithm records previous answers so that it can immediately fix a problem if it reappears. The search space could be kept from growing exponentially and processing cost might be decreased thanks to the paddock limitations that were developed.

The algorithm includes a search area where food particles are dispersed around the field and is thought to be the answer to the issue. In order to reduce the fitness function, the cattle, acting as the search agent, search the food particles in the paddock area. It is possible to express fitness as

$$FI_i = Yf_j - Xf_j \quad (1)$$

The search space expresses the food ingredients as

$$FP = \begin{bmatrix} fe_{11} & fe_{12} & \cdots & fe_{1n} \\ fe_{21} & fe_{22} & \cdots & fe_{2n} \\ \vdots & \vdots & \ddots & \vdots \\ fe_{m1} & fe_{m2} & \cdots & fe_{mn} \end{bmatrix} \quad (2)$$

The food particles in the solution space are taken to be the solutions for the given problem, with the only derived restrictions being the paddock area. It is possible to express the restrictions derived for choosing the best problem-solving strategy as

$$\begin{aligned} ll_1 < fe_{mn} > ul_1, \\ ll_2 < fe_{mn} > ul_2, \\ \dots \end{aligned}$$

$$ll_a < fe_{mn} > ul_b \quad (3)$$

The type of the problem determines how many limitations are there. The quantity of  $C_{best}$  solutions is found and there will be one greatest overall solution among them. One way to express the  $p_{best}$  solution count is

$$C_{best,i} = \begin{bmatrix} C_{11} & C_{12} & \dots & C_{1y} \\ C_{21} & C_{22} & \dots & C_{2y} \\ \vdots & \vdots & \ddots & \vdots \\ C_{x1} & C_{x2} & \dots & C_{xy} \end{bmatrix} \quad (4)$$

The food particle closest to the cow will first be chosen for the best overall solution. The food particle originally designated as the best in the world will be compared to the one at the place after the cattle has moved from its current position. Based on the weight of the food particle, comparisons are made. Two factors—distance and prey volume—will be used to calculate the weightage. The search agent's distance from the food particle will be taken into account. It is possible to express the distance  $D_i$  as

$$D_i = |Co - C_{xy}| \quad (5)$$

Where, 'Co' indicates the agent for searching. The second consideration is the volume of the food taken into account during the specific iteration, which is denoted by the symbol  $V_{fp}(i)$ . Finally, the total food particle weight can be conveyed as

$$W_{pbest,i} = D_i + V_{fp}(i) \quad (6)$$

The weightages are put in matrix storage and conveyed as,

$$W_{Cbest,i} = \begin{bmatrix} W_{C11} & W_{C12} & \dots & W_{C1n} \\ W_{C21} & W_{C22} & \dots & W_{C2n} \\ \vdots & \vdots & \ddots & \vdots \\ W_{Cm1} & W_{Cm2} & \dots & W_{Cmn} \end{bmatrix} \quad (7)$$

Initial responsibility for the selected solution for  $CG_{best} = C_{xy} \cdot C_{xy}$  indicates the food particle that is currently there. The next place can express the food particle as  $fC_{l+1}$ .

The  $CG_{best}$  solution will still be used, if the  $C_{xy}$ 's weight is greater than  $C_{xy+1}$ . The weight of the  $C_{xy}$  will be designated as the " $CG_{best}$  solution" if it is less than the weight of the  $C_{xy+1}$ . The best answer overall, or the optimal solution, can also be discovered among the many options.

#### Pseudo code for Cattle Grazing Pattern Optimization algorithm (CGPO)

1. Begin the search in space S
2. Set the lower band limit and upper band (UB) (LB)
3. Use Eqn (2) to determine FI
4. For n between 0 and I
5. Get  $FI(i)$
6.  $i = i + FI(i-1)$
7. UB=0
8. end
9. Examine the area for acceptable food particles (solution)
10. if  $lb_a < fC_{mn} > ub_b$
11.  $C_{best}$  solution using equation (4) to get the optimum answer
12. Use Eqn to calculate the distance  $D_i$  (5)
13. for  $i = 1$  to n.
14. Calculate the Weightage of all feasible options.
15. End
16. End
17. End

#### CNN-training norms

Iterative training is used in CNN. The network weights are changed to reduce the error between the actual network output and goal output for a particular sample at each iteration, which involves calculating the network outputs for one (or more) samples in the training set. In actuality, the error function is judged using a quadratic function, cross entropy, or any other mixed functional. Training is therefore reduced to reducing an error function.

- **Convolution layer**

The spatial relationships between the pixels are preserved through convolution. The computational or subsampling layer that follows each convolutional layer helps to shrink the size of the image by averaging the values of the local output neurons.

- **Subsampling with MAX-pooling layer**

By locally averaging the values of the output neurons, the subsampling layer zooms planes. Thus, a hierarchical structure is established. More widespread properties that are less dependent on image distortion are extracted from later levels. A convolution layer and a subsampling layer differ in that a convolution layer has nearby neurons' areas overlap it, whereas a subsampling layer does not.

The pooling layer scales the spatial volume using a maximum function and functions independently of the depth of the input data. The convolution network's architecture makes the assumption that the presence of a sign is more significant than knowledge of its location. As a result, the highest value is chosen from a group of nearby neurons in the feature map and is treated as a single neuron in the lower dimension feature map. Pooling layers can also do averaging subsampling or even L2-normalized subsampling in addition to maximum subsampling.

- **Dropout layer**

Different regularization approaches are used to prevent network retraining. A rapid and effective regularization technique called dropout involves randomly selecting a subnet during training from the network's aggregate structure. As a result, some neurons are blocked from participating in the process, and going forward, the scales are only updated in the designated subnet. Only the weights of the remaining neurons are changed as a result. The probability that each neuron will be removed from the network as a whole is known as the dropout rate. This layer cuts the period of one training session in half and, in comparison to traditional regularization strategies, enables the network to handle retraining more efficiently. This is due to the decreased number of optimized parameters.

- **Normalizing layer**

On this layer, the conventional normalization of inputs takes place (the sample average of their values is subtracted, and the result is divided by the root of the sample variance). The values at this layer's inputs from prior training iterations are taken into account for calculating the sampled values. With this method, the network can be learned more quickly, improving the outcome.

- **Fully connected layer**

This layer is a standard multilayer perceptron with categorization as its function. The quality of recognition is improved by optimizing the model's intricate nonlinear function. One neuron from the hidden layer is connected to each neuron on each map from the preceding subsample layer. As a result, the number of mappings in the subsample layer is the same as the number of neurons in the hidden layer. In a completely connected layer, neurons are coupled for every activation in the preceding layer, much like in regular neural networks. Matrix multiplication and biasing can be used to determine their activations. Convolutional layers differ from fully connected layers in that their neurons are only connected to the local area of the input and share parameters.

## RESULTS AND DISCUSSION

The experiment findings are reported in this section to support the efficacy of our method in detecting glaucoma and locating the diseased area. The LAG database is used for glaucoma detection. Among the 11,760 fundus images, there are 4,878 positive and 6,882 negative glaucoma samples. This LAG contributed by Beijing Tongren Hospital and the Chinese Glaucoma Study Alliance (CGSA)[30]. To demonstrate that the method does not over-fit, validation also makes use of the RIM-one database. Three decisions that are useful for constructing the CNN structure were reached as a result of the tiered grade system.

With 11,760 fundus photos in the LAG database, the experiment is put into practice. 10,928 of the 11,760 total photos are utilized for training, while 832 are used for testing. By three times garnering the fundus photos to 30%, 50%, and 70% of their original dimension, the training set photographs are enhanced. There is no subject or eye overlap and each sample is distinct. By testing it on a RIM-ONE, the suggested method's generalizability is confirmed. It is carefully set because the initial parameters have an impact on CNN detection.

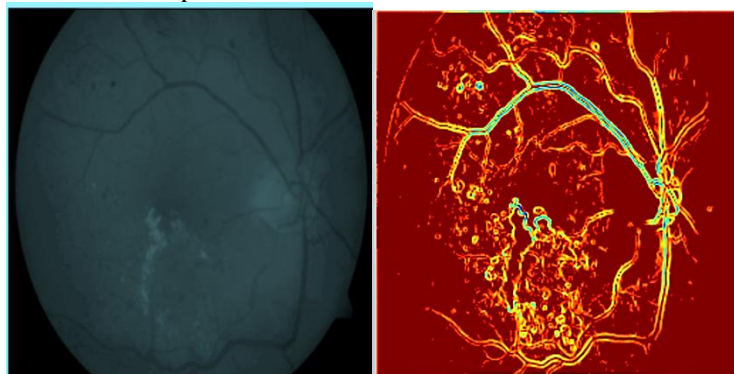


**Fig. 5** Input image and segmented pattern

Table 1 compares and contrasts our technique with eight existing heuristic glaucoma detection methods based on various variables. The measures that are used especially are SD (Standard deviation), Accuracy, specificity, sensitivity, DS (dice

similarity), and JD (Jaccard Distance). While the proposal has a higher rate of true positives and true negatives, it also has a smaller percentage of false positives and false negatives. Given the high accuracy of approximately 97% and the 0.05% deviation from the ground truth images, the PCOA was optimized with CNN. According to Table 2 and Fig. 6 (a-e), DS and JD calculate the percentage of similarity and dissimilarity among the output images and the ground truth images. About 97% of the ground truth's similarities and 4% of its differences were produced by the suggested approach. About 97% of the ground truth's similarities and 4% of its differences were produced by the suggested approach. Overall, the proposed approach outperforms the contrasted heuristic approaches in terms of performance.

**Table 1** Simulation comparison of heuristic segmentation approaches for glaucoma detection

Segmentation Approaches	Data set	Metrics							
		TP	FP	TN	FN	ACC	SD	DS	JD
Super pixel classification	LAG	0.76	0.15	0.84	0.23	88.0	0.20	0.84	0.20
	Rim-one	0.77	0	1.00	0.22	88.9	0.28	0.85	0.19
Contour based	LAG	0.78	0.14	0.85	0.21	88.8	0.20	0.85	0.19
	Rim-one	0.78	0	1.00	0.21	89.5	0.26	0.86	0.18
Region growing	LAG	0.78	0.13	0.86	0.21	89.2	0.20	0.86	0.18
	Rim-one	0.79	0	1.00	0.20	89.9	0.21	0.87	0.17
K-means Clustering	LAG	0.79	0.13	0.86	0.20	89.6	0.18	0.86	0.19
	Rim-one	0.80	0	1.00	0.19	90.0	0.19	0.87	0.17
Intuitionistic Fuzzy C-means clustering	LAG	0.80	0.12	0.87	0.19	90.3	0.17	0.88	0.16
	Rim-one	0.82	0	1.00	0.17	91.1	0.17	0.89	0.14
Spatial Fuzzy C-means clustering	LAG	0.81	0.11	0.88	0.18	90.7	0.18	0.89	0.15
	Rim-one	0.82	0	1.00	0.17	91.3	0.18	0.90	0.14
Adaptively regularized Kernel-based Fuzzy c means clustering	LAG	0.82	0.10	0.89	0.17	91.4	0.17	0.89	0.14
	Rim-one	0.84	0	1.00	0.15	92.4	0.17	0.90	0.13
Attention based CNN (base paper)	LAG	0.83	0.09	0.90	0.15	91.8	0.11	0.91	0.10
	Rim-one	0.85	0	1.00	0.12	93.0	0.15	0.92	0.09
RFSO on Attention based CNN	LAG	0.92	0.02	0.90	0.20	95.18	0.08	0.97	0.9
	Rim-one	0.94	0.01	0.90	0.15	94.24	0.04	0.95	0.7
PCOA on Attention based CNN	LAG	0.94	0.02	0.92	0.24	97.18	0.05	0.98	0.91
	Rim-one	0.96	0.02	0.92	0.12	96.12	0.03	0.98	0.81

**Table 2** Simulation comparison of CNN approaches for glaucoma detection

Database	Method	Accuracy				Sensitivity				Specificity			
		1	2	3	4	1	2	3	4	1	2	3	4
LAG	Chen et al	85.4	85.2	88.6	89.2	83.2	85.1	87.12	89.4	80.0	60.2	65.3	89.0
	Li et al	86.5	89	90	89.7	88.3	89.1	90.25	91.4	67.8	61.3	63.25	88.4
	Li, L et al	92.1	90	95.34	96.2	91.1	92.5	94.3	95.4	85.2	75.2	78.2	96.7
	Proposed	98.1	96	98.77	98.12	90.11	92.12	95.67	96.92	90.12	91.57	90.44	98.43
RIM-ONE	Chen et al	82.3	83.2	75	80.0	60.2	65.3	67.45	69.6	83.2	85.1	87.12	87.0
	Li et al	86.4	85.1	65	67.8	61.3	63.25	65.4	67.4	88.3	89.1	90.25	68.1
	Li, L et al	92.63	86.9	72.16	85.2	75.2	78.2	82.6	84.8	91.1	92.5	94.3	85.5
	Proposed	98.12	96.12	94	90.92	91.76	90.89	91.45	90.12	91.43	93.78	94.43	90.89

Database	Method	AUC				F1 Score			
		1	2	3	4	1	2	3	4
LAG	Chen et al	0.91	0.92	0.93	0.953	0.84	0.85	0.89	0.886
	Li et al	0.92	0.95	0.954	0.960	0.85	0.89	0.91	0.954
	Li, L., et al	0.92	0.95	0.98	0.983	0.88	0.90	0.93	0.954
	Proposed	0.95	0.95	0.97	0.99.12	0.94	0.99	0.98	0.98
RIM-ONE	Chen et al	0.75	0.78	0.82	0.831	0.65	0.68	0.69	0.711
	Li et al	0.65	0.68	0.72	0.731	0.61	0.63	0.65	0.654
	Li, L., et al	0.81	0.85	0.89	0.916	0.81	0.82	0.825	0.837
	Proposed	0.96	0.94	0.94	0.94	0.912	0.94	0.	0.94

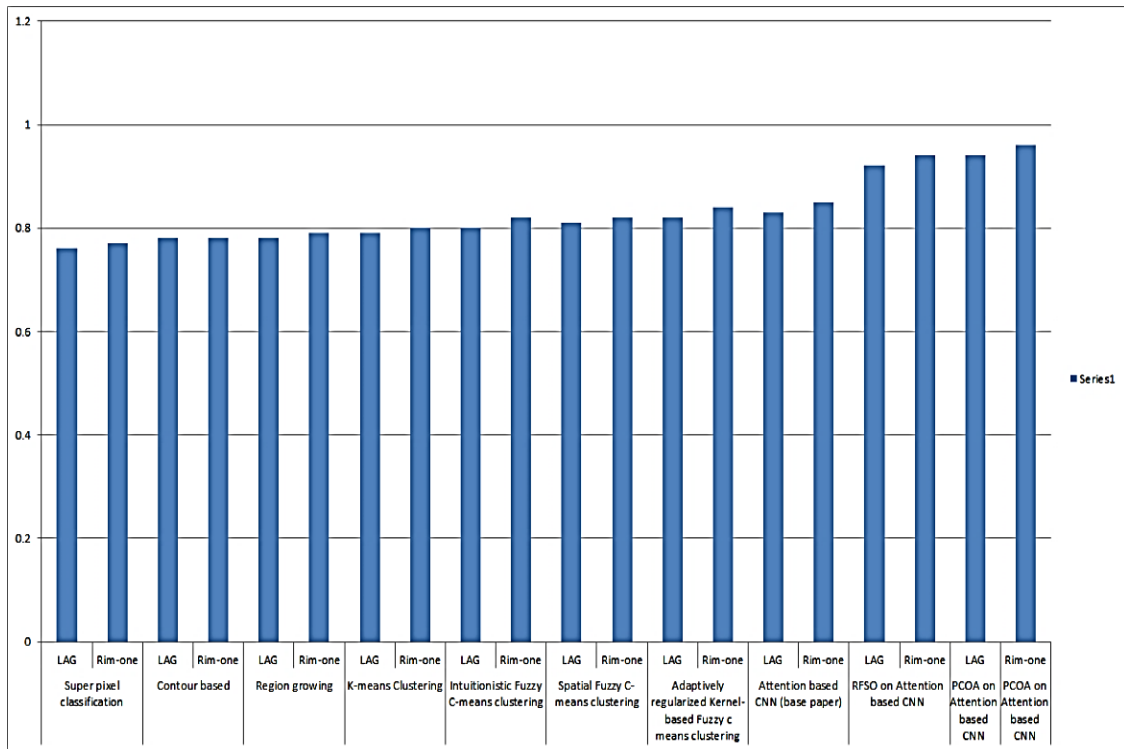


Fig. 6 (a) The performance comparisons of TP for several classifiers

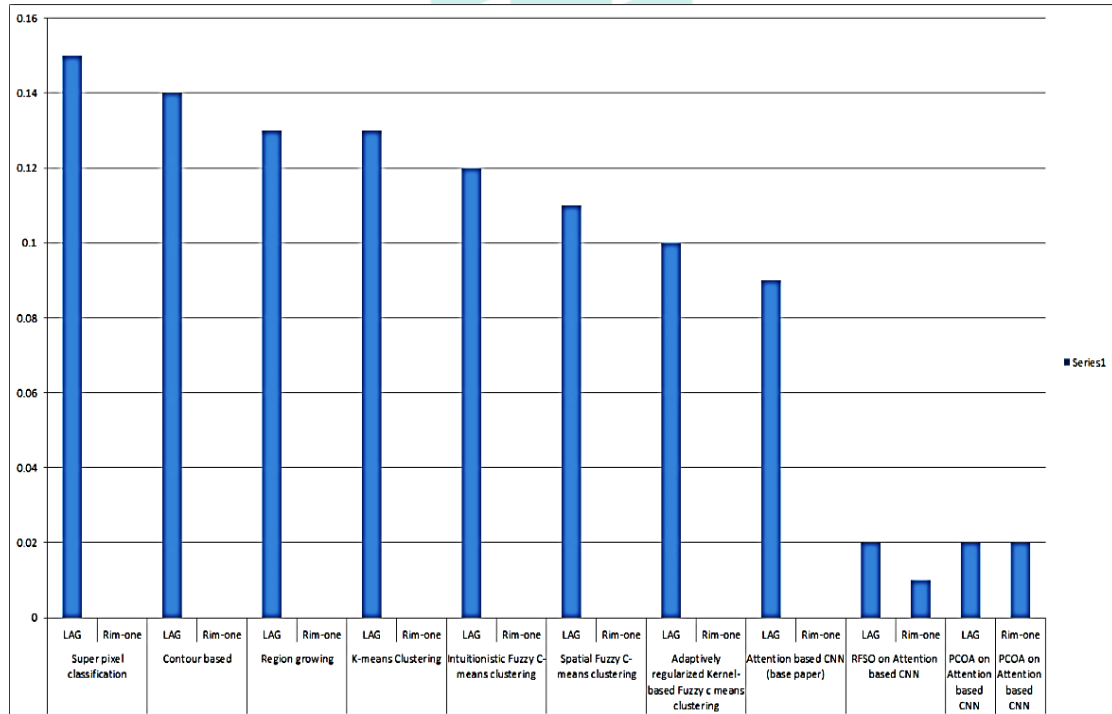


Fig. 6 (b) The performance comparisons of TN several classifiers

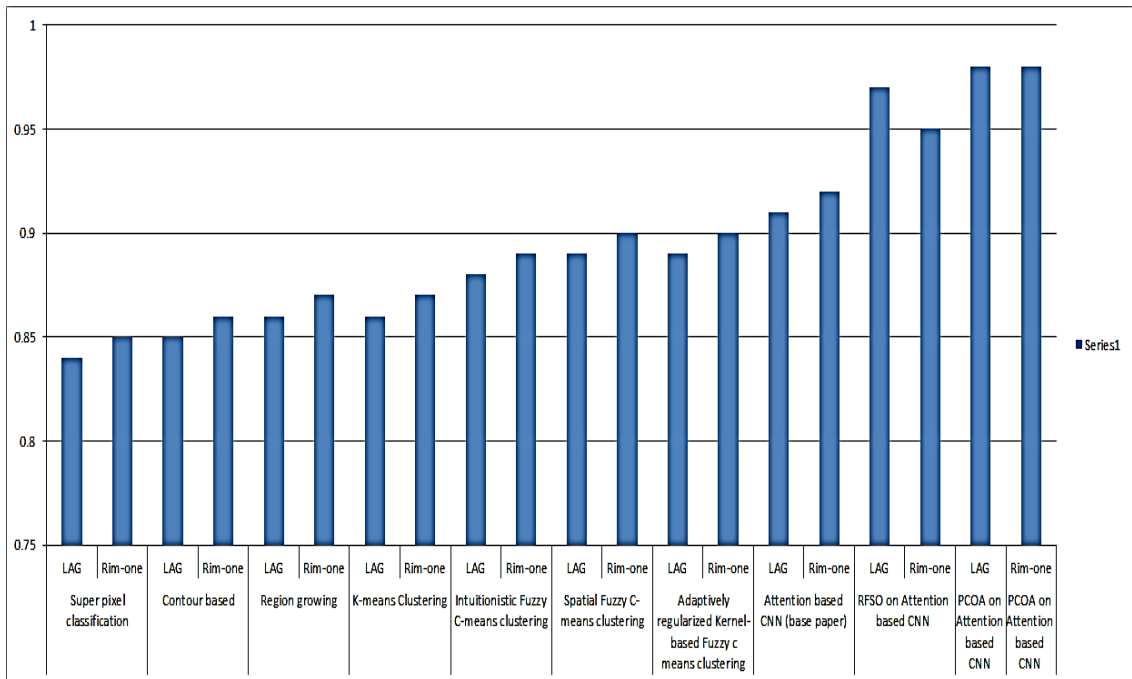


Fig. 6 (c) The performance comparisons of DS for several classifiers

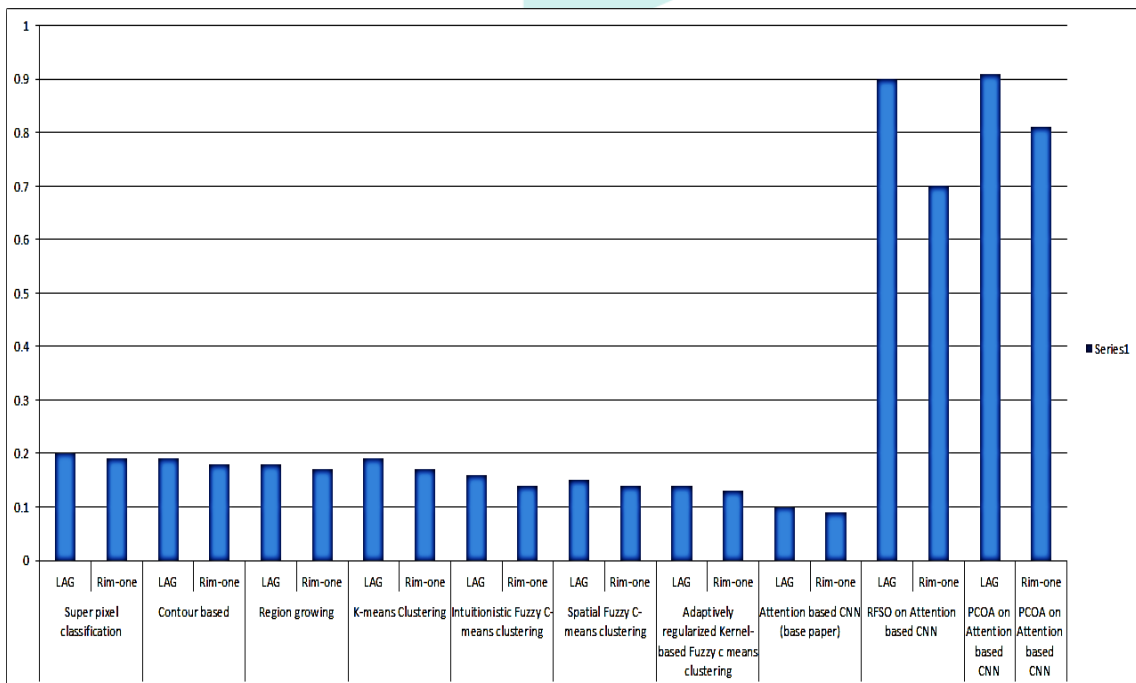
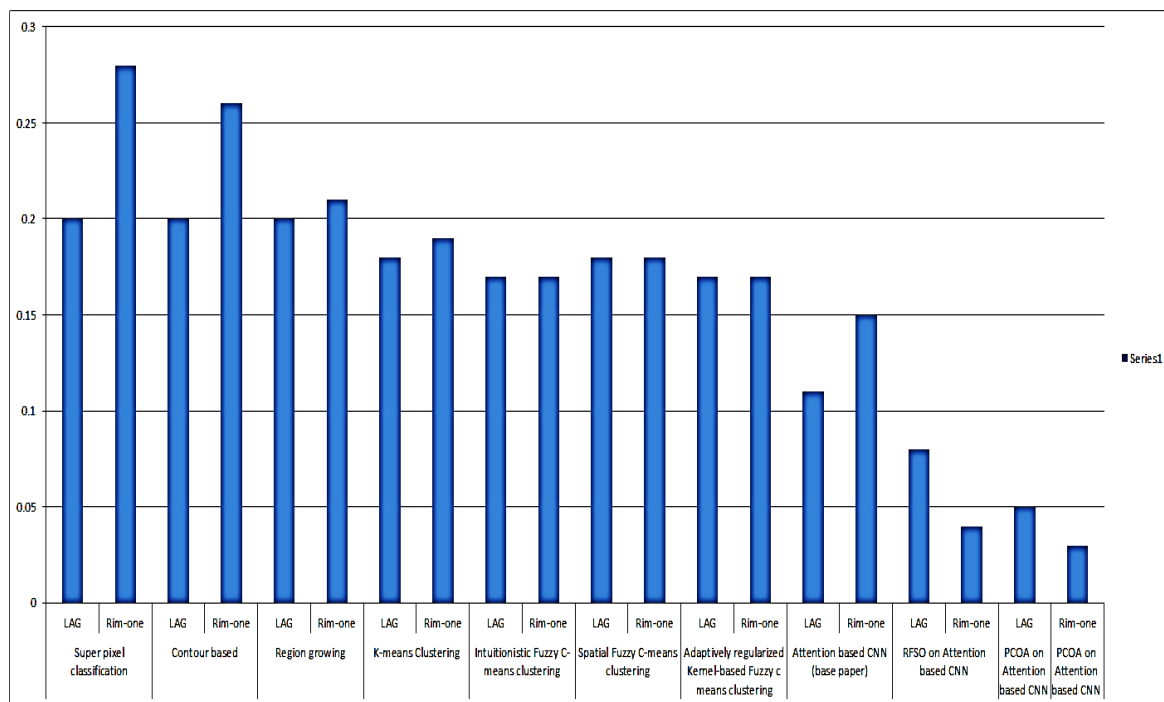


Fig. 6 (d) The performance comparisons of JD for several classifiers



**Fig. 6 (e)** The performance comparisons of SD for several classifiers  
**Fig. 6 (a-e)** The performance comparisons of simulated parameters for several classifiers

The compared parameters are true positive (TP), true negative (TN), standard deviation (SD), JD, and DS  $F_2$  Score as plotted in Fig. 6. From these figures (a-e), the proposed PCOA optimizer provides the better progress, when compared to the relevant approaches in our studies.

## Discussion

The experiment utilized the LAG database, containing a significant number of fundus images, for glaucoma detection. Additionally, validation was conducted using the RIM-one database to ensure the method's generalizability and avoid over fitting. This approach reflects a comprehensive evaluation strategy, ensuring robustness and reliability in the results. Table 1 presents a comparative analysis of the proposed PCOA method with eight existing heuristic segmentation approaches for glaucoma detection. Metrics such as accuracy, specificity, sensitivity, dice similarity (DS), and Jaccard Distance (JD) were used for evaluation. The proposed method demonstrates superior performance across various metrics, indicating its effectiveness in accurately detecting glaucoma features compared to existing approaches. Table 2 further compares the performance of CNN approaches for glaucoma detection using different databases. Metrics such as accuracy, sensitivity, specificity, area under the curve (AUC), and F1 score were evaluated. The proposed PCOA method consistently outperforms existing CNN approaches, achieving higher accuracy and sensitivity levels, which are crucial for reliable glaucoma detection. Figs. 6 (a-e) provide visual representations of the performance comparisons for true positive (TP), true negative (TN), standard deviation (SD), JD, and DS  $F_2$  Score across various classifiers. The plots clearly demonstrate the superior progress achieved by the PCOA optimizer compared to relevant approaches in the study, reaffirming the efficacy of the proposed method. The findings of this study highlight the effectiveness of the PCOA method in enhancing glaucoma detection accuracy and efficiency. By optimizing CNN classifiers using PCOA, the method achieves high levels of accuracy and sensitivity, critical for early diagnosis and intervention in glaucoma cases. These results have significant implications for improving clinical outcomes and patient care in the field of ophthalmology. Moving forward, the proposed PCOA method holds promise for further advancements in automated glaucoma detection technology. Future research could focus on refining the optimization process, exploring additional datasets, and integrating emerging technologies to enhance the method's performance and applicability in real-world clinical settings.

## CONCLUSION

The pulikulam Cattle Optimization method (PCOA), a new bio-inspired algorithm for the optimization process is introduced in this research. By activating the particular parameters, this optimization procedure can be used in any field to improve the results. The dietary habits of cattle are taken into account in the PCOA module. The search space is allocated by taking into account the population of the grass grown in the paddock in order to acquire the solution set for the specified optimization. The grasses that the cattle choose to eat from this field are then thought to be the best choice. This algorithm allows for the acquisition of a number of solutions sets via the route travelled by the cattle to consume the grass. This type of newly introduced optimizer provides the better optimum value to tune the parameters of CNN classifier. Hence, it classifies the glaucoma disease effectively than other previously evaluated optimizers.

## REFERENCES

1. Németh, J., Tóth, G., Resnikoff, S. and de Faber, J.T., 2019. Preventing blindness and visual impairment in Europe: What do we have to do?. *European journal of ophthalmology*, 29(2), pp.129-132.
2. Bhargava, S., Mason, L. and Okeke, C., The Significance of Screening Family Members in Glaucoma: Opportunities and Challenges. *Journal of Glaucoma*, pp.10-1097.
3. Zhang, Z., Lee, B.H., Liu, J., Wong, D.W.K., Tan, N.M., Lim, J.H., Yin, F., Huang, W., Li, H. and Wong, T.Y., 2010, June. Optic disc region of interest localization in fundus image for glaucoma detection in ARGALI. In *2010 5th IEEE Conference on Industrial Electronics and Applications* (pp. 1686-1689). IEEE.
4. Hussain, S.A. and Holambe, A.N., 2015. Automated detection and classification of glaucoma from eye fundus images: a survey. *International Journal of Computer Science and Information Technologies*, 6(2), pp.1217-1224.
5. Bock, R., Meier, J., Nyúl, L.G., Hornegger, J. and Michelson, G., 2010. Glaucoma risk index: automated glaucoma detection from color fundus images. *Medical image analysis*, 14(3), pp.471-481.
6. Nayak, J., Acharya U, R., Bhat, P.S., Shetty, N. and Lim, T.C., 2009. Automated diagnosis of glaucoma using digital fundus images. *Journal of medical systems*, 33, pp.337-346.
7. Acharya, U.R., Dua, S., Du, X. and Chua, C.K., 2011. Automated diagnosis of glaucoma using texture and higher order spectra features. *IEEE Transactions on information technology in biomedicine*, 15(3), pp.449-455.
8. Agarwal, A., Gulia, S., Chaudhary, S., Dutta, M.K., Travieso, C.M. and Alonso-Hernández, J.B., 2015, June. A novel approach to detect glaucoma in retinal fundus images using cup-disk and rim-disk ratio. In *2015 4th international work conference on bioinspired intelligence (IWOBI)* (pp. 139-144). IEEE.
9. Mookiah, M.R.K., Acharya, U.R., Lim, C.M., Petznick, A. and Suri, J.S., 2012. Data mining technique for automated diagnosis of glaucoma using higher order spectra and wavelet energy features. *Knowledge-Based Systems*, 33, pp.73-82.
10. Kumar, B.N., Chauhan, R.P. and Dahiya, N., 2018, February. Detection of glaucoma using image processing techniques: a critique. In *Seminars in ophthalmology* (Vol. 33, No. 2, pp. 275-283). Taylor & Francis.
11. Almazroa, A., Burman, R., Raahemifar, K. and Lakshminarayanan, V., 2015. Optic disc and optic cup segmentation methodologies for glaucoma image detection: a survey. *Journal of ophthalmology*, 2015.
12. Schacknow, P.N. and Samples, J.R. eds., 2010. *The glaucoma book: a practical, evidence-based approach to patient care*. Springer Science & Business Media.
13. Poshtyar, A., Shanbehzadeh, J. and Ahmadi, H., 2013, December. Automatic measurement of cup to disc ratio for diagnosis of glaucoma on retinal fundus images. In *2013 6th International Conference on Biomedical Engineering and Informatics* (pp. 24-27). IEEE.
14. Vlachokosta, A.A., Asvestas, P.A., Matsopoulos, G.K., Uzunoglu, N. and Zeyen, T.G., 2007, August. Preliminary study on the association of vessel diameter variation and glaucoma. In *2007 29th Annual International Conference of the IEEE Engineering in Medicine and Biology Society* (pp. 888-891). IEEE.
15. Tham, Y.C., Li, X., Wong, T.Y., Quigley, H.A., Aung, T. and Cheng, C.Y., 2014. Global prevalence of glaucoma and projections of glaucoma burden through 2040: a systematic review and meta-analysis. *Ophthalmology*, 121(11), pp.2081-2090.
16. Weinreb, R.N., Aung, T. and Medeiros, F.A., 2014. The pathophysiology and treatment of glaucoma: a review. *Jama*, 311(18), pp.1901-1911.
17. Esteva, A., Kuprel, B., Novoa, R.A., Ko, J., Swetter, S.M., Blau, H.M. and Thrun, S., 2017. Dermatologist-level classification of skin cancer with deep neural networks. *nature*, 542(7639), pp.115-118.
18. Harmon, S.A., Sanford, T.H., Xu, S., Turkbey, E.B., Roth, H., Xu, Z., Yang, D., Myronenko, A., Anderson, V., Amalou, A. and Blain, M., 2020. Artificial intelligence for the detection of COVID-19 pneumonia on chest CT using multinational datasets. *Nature communications*, 11(1), p.4080.
19. Gulshan, V., Peng, L., Coram, M., Stumpe, M.C., Wu, D., Narayanaswamy, A., Venugopalan, S., Widner, K., Madams, T., Cuadros, J. and Kim, R., 2016. Development and validation of a deep learning algorithm for detection of diabetic retinopathy in retinal fundus photographs. *Jama*, 316(22), pp.2402-2410.
20. Burlina, P.M., Joshi, N., Pacheco, K.D., Freund, D.E., Kong, J. and Bressler, N.M., 2018. Use of deep learning for detailed severity characterization and estimation of 5-year risk among patients with age-related macular degeneration. *JAMA ophthalmology*, 136(12), pp.1359-1366.
21. Dong, Y., Zhang, Q., Qiao, Z. and Yang, J.J., 2017, October. Classification of cataract fundus image based on deep learning. In *2017 IEEE international conference on imaging systems and techniques (IST)* (pp. 1-5). IEEE.
22. Tan, N.Y., Friedman, D.S., Stalmans, I., Ahmed, I.I.K. and Sng, C.C., 2020. Glaucoma screening: where are we and where do we need to go?. *Current opinion in ophthalmology*, 31(2), pp.91-100.
23. Hemelings, R., Elen, B., Barbosa-Breda, J., Lemmens, S., Meire, M., Pourjavan, S., Vandewalle, E., Van de Veire, S., Blaschko, M.B., De Boever, P. and Stalmans, I., 2020. Accurate prediction of glaucoma from colour fundus images with a convolutional neural network that relies on active and transfer learning. *Acta ophthalmologica*, 98(1), pp.e94-e100.
24. Thompson, A.C., Jammal, A.A. and Medeiros, F.A., 2019. A deep learning algorithm to quantify neuroretinal rim loss from optic disc photographs. *American journal of ophthalmology*, 201, pp.9-18.
25. Sophia, S.S.S.J. and Diwakaran, S., 2023. Hybrid muzzy electric fish and grasshopper optimization algorithm (MEF-GOA) based CNN for detection and severity differentiation of glaucoma in retinal fundus image. *Journal of Intelligent & Fuzzy Systems*, 44(2), pp.2285-2303.
26. Wang, Y., Yuan, Y. and Lei, Z., 2020. Fast SIFT feature matching algorithm based on geometric transformation. *IEEE Access*, 8, pp.88133-88140.
27. Kun, Z., Xiao, M. and Xinguo, L., 2019. Shape matching based on multi-scale invariant features. *IEEE Access*, 7, pp.115637-115649.
28. Meng, X., Liu, Y., Gao, X. and Zhang, H., 2014. A new bio-inspired algorithm: chicken swarm optimization. In *Advances in Swarm Intelligence: 5th International Conference, ICSI 2014, Hefei, China, October 17-20, 2014, Proceedings, Part I 5* (pp. 86-94). Springer International Publishing.

29. Werner, J., Umstatter, C., Kennedy, E., Grant, J., Leso, L., Geoghegan, A., Shalloo, L., Schick, M. and O'Brien, B., 2019. Identification of possible cow grazing behaviour indicators for restricted grass availability in a pasture-based spring calving dairy system. *Livestock science*, 220, pp.74-82.
30. Li, L., Xu, M., Liu, H., Li, Y., Wang, X., Jiang, L., Wang, Z., Fan, X. and Wang, N., 2019. A large-scale database and a CNN model for attention-based glaucoma detection. *IEEE transactions on medical imaging*, 39(2), pp.413-424.
31. Valarmathi, S. and Vijayabhanu, R., 2022. Computer-Aided Diabetic Retinopathy Diagnosis Using Conventional and Deep Learning Techniques—A Comparison. In *Advance Concepts of Image Processing and Pattern Recognition: Effective Solution for Global Challenges* (pp. 131-153). Singapore: Springer Singapore.
32. Coan, L.J., Williams, B.M., Adithya, V.K., Upadhyaya, S., Alkafri, A., Czanner, S., Venkatesh, R., Willoughby, C.E., Kavitha, S. and Czanner, G., 2023. Automatic detection of glaucoma via fundus imaging and artificial intelligence: A review. *Survey of ophthalmology*, 68(1), pp.17-41.

